Survivability Analysis of a Two-Tier Heterogeneous Cellular Network

Lang Xie[1], Poul E Heegaard, Yuming Jiang

Department of Telematics, Norwegian University of Science and Technology (NTNU)

[a]NO-7491, Trondheim, Norway

Abstract

Network design and operation of a mobile network infrastructure, especially its base station systems, need to consider survivability as a fundamental requirement. To this end, quantifiable approaches to survivability analysis of such infrastructures are crucial. The objective of this paper is to propose a model for quantification of the survivability of wireless communication networks subject to massive failures, e.g., caused by natural disasters, common mode hardware and software failures, and security attacks. This means to analyze the transient behavior of the recovery phases. We use a Markov model approach, and apply this in a case study of a two-tier infrastructure-based wireless network. To take location information of base stations into consideration, the spatial average network performance is estimated by means of a stochastic geometry based approach. Further, in order to avoid state space explosion while addressing large networks, an approximate product-form analysis approach is also presented, where the two base stations tiers are decoupled such that their survivability analysis can be studied independently. The assumptions used in the proposed models, including Poisson point process (PPP) assumption and product-form decomposition assumption, are validated on real data. Numerical experiments are also performed to investigate the approximation accuracy and computational efficiency of the product-form analysis approach, as well as to examine the effect of different parameters on the network's survivability. The results show that

---

[1]Lang Xie is the corresponding author with email address langxie_77@163.com.

the approximate product-form approach is more scalable with reasonably good accuracy and hence may be more preferred for analysis of large size networks.

Keywords: survivability, analytical models, disastrous failures, product-form approximation

---

1. Introduction

1.1. Motivation

With the explosive growth of mobile usage around the world, wireless communications plays a fundamental role in supporting effective coordination between first responders and victims in case of disasters. Since mobile networks are to be relied upon as a critical communication infrastructure, their survivability to disasters must be maximized. Following a disaster, critical infrastructure issues affecting a mobile network often include a loss of base station (BS) due to damage to the station itself (or the transmission), lack of power and logistics issues. Although other network elements should not be ignored, BSs are often the most vulnerable part of the whole infrastructure under natural disasters such as hurricane, earthquake, tsunami, etc., or human-made disasters such as massive Distributed Denial of Service (DDoS) attacks. When a disaster strikes, it may affect a large region of areas causing multiple failure of BSs located in those areas (e.g., [1],[2],[3]). Under such a case, mobile network operators (MNOs) face many challenges to ensure continuous network operation.

Since restoring the mobile network to operational levels as soon as possible after a disaster is critical, MNOs have increasingly invest in their disaster response toolkits. For example, KDDI of Japan has taken a set of measures associated with ensuring network reliability during disasters, such as back-up communication modes for the dissemination of warnings and other critical information. One of the fastest methods of restoring damaged cellular network is constructing emergency communication network (ECN) with the rapid deployment of temporary and portable cell sites. For example, NTT of Japan has proposed a Deployable Base Stations (DBSs)-based ECN to be deployed after

2

a disaster occurs. Users can use the DBS to send messages from a disaster area [4]. Vodafone Foundation proposes an Instant Network Solution to enable e-mergency communications in disaster areas through the deployment of portable mobile GSM BSs. It is able to deliver voice and SMS connectivity to areas that are not normally connected. By deploying DBSs on an partially damaged cellular network, a two-tier heterogeneous network (HCN) is formed with two types of BSs, macro cellular BSs (MBSs) and DBSs.

In general, lightweight (DBSs)-based ECN solutions are desired by all M-NOs to enhance their network's ability to continuously deliver services under failures. However, survivability evaluation of different (DBSs)-based ECN solutions is still an ongoing research problem. This is not only because of the size and complexity of the problem, but also because the quantifiable approaches of survivability are lacking. In order to evaluate the survivability of such overlay networking accurately and tractably, it is essential to develop effective models for assessing the network performance during the (transient) period that starts after a failure till the system fully recovers. The resulting survivability modeling and analysis provides a promising new direction for mobile network design to avert the impact of geographical disasters or attacks.

1.2. Related work

Geographically correlated failures have been considered in survivability and vulnerability assessment of optical backbone networks with preplanning [5],[6] or reactive routing protocols [7]. In many prior works, the objective is to find the most vulnerable network area of a predefined size, under specific disaster models, e.g., under line disasters [8], circular disasters [8],[9], or general polygon disasters [10]. For all the network components that intersect the disaster, they may become definitely inoperative [5],[8] or fail with a probability [9],[11]. How-ever, the research of survivability under geographically correlated failure has been less conducted on wireless access networks. Evaluating survivability of BS system against disaster is very complicated and challenging due to the problem complexity and the limitation in scalability, in particular for a heterogeneous

3

networking scenario consisting of different types of BSs.

In order to accurately estimate the network's survivability performance, it is critical to take into account the spatial placement of BSs, since, as highlighted above, a disaster strike may affect a large region of areas causing failure of BSs in those areas. Generally, wireless network deployment can be modelled as a collection of points distributed on a two-dimensional plane. Each point, representing a wireless transceiver, is assigned wireless network related properties, such as downlink transmit power and operational frequency. Then, the average performance experienced by a user of such a network may be obtained either using stochastic geometry or through computer simulations. In stochastic geometry a typical assumption is to use a homogeneous Poisson point process (PPP) to represent network deployment, while in computer simulations the hexagonal lattice model is used. PPP has been widely used in performance evaluation of large-scale wireless network due to its simplicity and tractability [12]. Also research has shown that the PPP model is accurate when compared to actual BS deployment [13], [14]. Networks will continue to become increasingly heterogeneous as we move toward 5G [15]. Heterogeneous cellular networks (HCNs) can be a key element for emergency communications. This novel networking paradigm is based on the idea of deploying short-range, low-power, and low-cost BSs that operate in conjunction with the main 5G macro cellular network infrastructure. A heterogeneous small cell network with overlay small cells and macrocell is a promising solution to enhance service survivability of mobile networks in large-scale failure scenarios [16]. Modeling BS deployment patterns in multiple-tier heterogeneous cellular network scenarios have been studied in [17], [18]. Most of the stochastic geometry works on HCNs focus on the spatial average performance of the network, but neglects the temporal dynamics due to disaster failure. Our work differentiates with previous work in that we are interested in modeling the temporal dynamics of the network performance, not only a "snapshot" of one time instant.

V. Jindal et al. [19] analyzes the disaster survivability of a cellular network from a truncated continuous time Markov chain (CTMC) model. In this work,

4

the transient performance variation of system from a failure to the normal mode is taken into account as suggested by T1A1.2 definition [20]. However, the main entity in the proposed models in both [16] and [19] is the individual BS rather than the whole network. A direct extension of the model to network-level will cause state space explosion issues in solving results from the model.

In order to avoid state space explosion while addressing large networks, a decomposition approach has been introduced [21]. This approach first decouples the models in space by analyzing the nodes independently and then decouples the performance and recovery models in time. The results show very good correspondence in performance metrics between the analytic approximations and the simulation results. However, in [21], spatial information of BSs is not taken into special account in the modeling and analysis. Specifically in [21] and other works, when analyzing the impact of large-scale failures caused by one external disturbance, the information used is often from just one "snapshot" of temporal spatial network statuses, which limits the use of a more complete temporal-spatial model of network nodes in the analysis.

1.3. Contributions

In this paper, we conduct quantitative, model-based analysis of the survivability of a two-tier HCN, which is formed by an ECN overlaid on an existing cellular network that is subject to disastrous breakdowns. Specifically, the focus is on characterizing the transient recovery behavior of HCN in the presence of disastrous failures. The recovery behavior of the network is modeled as a Markov chain, based on which the analysis is performed. To take into account the inter-tier spatial dependence of BSs in the performance modeling, the two types of BSs, MBSs and DBSs deployment in the above HCN are modeled as a PPP and a Poisson hole process (PHP), respectively. The spatial average network performance is estimated and viewed as a reward process on the Markov model. In addition, to help reduce the computation complexity, a product-form decomposition approach is performed in the Markov models. The performance formulas used in the proposed models are validated against Monte

5

Carlo simulation. Numerical experiments are also performed to investigate the approximation accuracy and computational efficiency of the product-form analysis approach against the exact analysis, as well as to examine the effect of different parameters on the network's survivability. The experimental results show that the product-form approximation provides tractable and reasonably accurate analysis of survivability performance.

The contribution of this paper are summarized as follows:

- The comprehensive spatial modeling of a two-tier HCN, which is formed by an ECN overlaid on a partially destructed cellular network is considered. By extending the results in [18] based on the features of the PPP and PHP, we conduct mathematical analysis and evaluation of the conditional coverage probability, per-user coverage and service unavailability of the above HCN. We present the equations and the detailed derivations for these measures and show how they depend on the system parameters. To the best of our knowledge, this is the first attempt to apply stochastic geometry into network survivability modeling.

- We present a Markov chain model that supports the survivability assessment of the above 2-tier HCN during the period that starts after a failure till the system fully recovers. Further, in order to avoid state space explosion while addressing large networks, an approximate product-form analysis approach is also presented.

- The correctness of the performance formulas used in the proposed models are validated against Monte Carlo simulation. We provide a realistic numerical study on the the approximation accuracy and computational efficiency of the product-form analysis approach against the exact analysis. The effect of different Markov model parameters on the network's survivability are also studied.

The rest of this paper is organized as follows: In Section 2, the system model and notations are given. Section 3 presents the survivability analysis in

6

detail, where the mathematical analysis of network performance is conducted in Section 3.2 and a product-form approximation approach is introduced in Section 3.4 to reduce the computation complexity. Section 4 presents validation and numerical results, which include validation of the performance formulas and the assumptions used in the proposed models in Section 4.1, and numerical results in Section 4.2, demonstrating the analytical results and the effect of different model parameters on survivability. Finally, a summary of this work is given in Section 5.

2. System Models

2.1. Overall Model

Consider the down-link communication in a network formed by a ECN overlaid on an existing cellular network , which are located in a certain urban area $\mathcal{A}_0$. The main cellular network is stroked by a large-scale disaster, and a portion of MBSs are damaged. As illustrated in Figure 1, the ECN is established via deployment of a number of DBSs to fill the coverage holes due to MBSs failure. Thus, the resulting two-tier HCN includes two types of BSs, i.e., MBSs and DBSs.

As our goal is to investigate the survivability performance under different resource conditions from a higher abstraction level, the Poisson point process (PPP) is adopted as the spatial model for the locations of MBSs. Although PPP-based models may not be realistic, they can provide closely exact performance results compared with the real BS deployment [13],[14]. The spatial distribution of the MBSs is modeled by a homogeneous PPP $\Phi_m = \{x_1, x_2, \cdots\} \subset \mathcal{A}_0$ of density λ_m. Under the strike of a disaster, we argue that the affected BSs should not always be inoperative, but may fail with a probability. We propose a probabilistic disaster damage ratio denoted γ $(0 < \gamma < 1)$ that represents the percentage of the damaged MBSs over the total number of original MBSs in the disaster-affected area. γ can be a function of external disaster, terrain, and network component fragility. Here, for the sake of tractability we assume γ is a
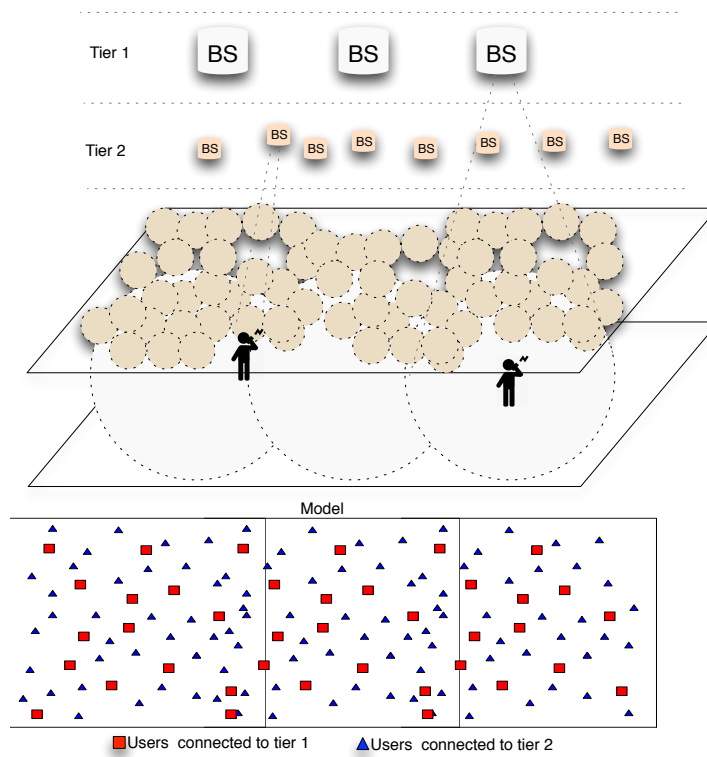
7

Figure 1: Illustration of a two-tier infrastructure wireless network utilizing two classes of BSs.

uniform random variable independent from MBS location. Thus, in case that a disaster has occurred, a thinning factor of $(1 - \gamma)$ will affect the original MBSs density, and the resulting new density will become $(1 - \gamma)\lambda_m$. Such implicit assumption of the random BS failure is due to the inherited random nature of the effect of disasters.

One of the fastest methods of restoring networks is the rapid deployment of DBSs. Deploying additional BSs can either reduce local network congestion or plug gaps in a damaged network. In order to reduce the interference and enhance the coverage, deployment of DBSs should consider repulsion characteristic existing among different tiers BSs. In this context, we assume that each MBS has an exclusion region, which is a disk with radius D centered at the location of MBS. DBSs are only deployed outside the exclusive region to fill the coverage holes. Under this setup, the DBSs form a Poisson hole process (PHP), which has been defined in [18]:

Definition 1. (Poisson Hole Process, PHP): Let Φ_m be a PPP of spatial density λ_m and $\tilde{\Phi}_d$ be a PPP of spatial density $\tilde{\lambda}_d > \lambda_m$. For each $x \in \Phi_m$, remove all the points in $\tilde{\Phi}_d \bigcap b(x, D)$, where $b(x, D)$ is a ball centered at x with radius D. Then the remaining points of $\tilde{\Phi}_d$ form the Poisson hole process Φ_d with spatial density $\lambda_d = \tilde{\lambda}_d \exp(-\lambda_m \pi D^2)$.

Let the potential locations of the DBSs follow a homogeneous PPP $\tilde{\Phi}_d = \{y_1, y_2, \cdots\} \subset \mathcal{A}_0$ of density λ_d. Then the actual locations of the DBSs follow a PHP of density $\lambda_d = \tilde{\lambda}_d \exp(-\lambda_m \pi D^2)$. We assume that each of BSs within the same tier have the same transmission power, which we denote P_m for MBSs and P_d for DBSs. The path loss is represented in Eq. (1)

$$l(x) = (G|x|)^{-\alpha}, \tag{1}$$

where constants $G > 0$ and $\alpha > 0$. G is a constant to merge constant parameters together. More specifically, the COST Walfisch-Ikegami model is taken for path loss as shown in $L = 42.6 + 26\log(d/1km) + 20\log(f/1\text{MHz})$ and the constant parameters are merged in G with a non-dB form [22]. Since our area of interest $\mathcal{A}_0$ is urban area, we choose COST 231 Walfisch-Ikegami Model that considers

9

the buildings in the vertical plane between the transmitter and the receiver.

The path loss model can be redefined depending upon the application scenario. We consider Rayleigh fading between each user and the serving BS. The fading (power) between a BS x and the typical user is denoted by h_x. The impact of fading follows the exponential distribution, i.e., that the generic fading variable h_x is exponential, with $\mathbb{E}[h_x] = 1$. In addition, the additive white Gaussian noise (AWGN) power is assumed to be a constant $\sigma^2 > 0$. The signal-to-interference-and-noise-ratio (SINR) thresholds for MBSs and DBSs are β_m, β_d, respectively.

As suggested in [18], the radius D of the exclusion region of MBS at x is chosen as $D = \zeta x (\frac{\eta_d P_d}{\eta_m P_m})^{\frac{1}{\alpha}}$ where ζ is a cell range expansion factor, P_m and P_d are transmit power of MBS and DBS, respectively, η_m and η_d are interference mitigation factor of MBS and DBS, respectively. It is intuitive that D should be proportional to the distance between the serving MBS and its user and the transmission power of the DBSs, and inversely proportional to the transmission power of the MBSs. Here, the definition of D differs from that of [18] in considering the coordination and interactions among the BSs. In order to guarantee the network's proper operation, intercell interference coordination (ICIC) techniques are required. In this paper, we approximate the reduction in the downlink interference due to this ICIC capability by the constant factor η_m, η_d for MBSs and DBS, respectively.

For resource allocation, we assume an orthogonal partitioning of resources, e.g., time-frequency resource blocks in orthogonal frequency division multiple access (OFDMA) which has been widely used in UMTS, LTE. We assume that each of MBSs and DBSs has N_b resource blocks and allocates at most one resource block to one user at a time. This assumption can be easily relaxed to incorporate users requiring more resource blocks, but this case is not in the scope of this paper. Users are assumed to follow a homogeneous PPP Φ_u with density λ_u across this area of interest and supported to access both MBSs and DBSs. Under this setup, the users located within D of an MBS get served by MBSs within that distance, i.e., a fraction of $k_m = 1 - \exp(-\lambda_m \pi D^2)$ of the users will be served by MBSs, and the rest are served by DBSs.

10

Table 1: Notation Summary

Notation	Description
$\mathcal{A}_0$	the geographic area of interest
Φ_m, λ_m	the spatial point porcess of MBSs and its density
Φ_d, λ_d	the spatial point porcess of DBSs and its density
λ_u	the density of users
γ	the ratio of damaged MBSs
P_m, P_d	the transmit power of MBSs and DBSs
β_m, β_d	the SINR threshold of MBSs and DBSs
α	the standard power-law path loss exponent

Table 1 summarizes the notations used in this paper.

2.2. Failure and Recovery Description

The above section concentrates more on the spatial modeling of the system. This section discusses the temporal behaviors of the system, during the period that starts after a failure till the system fully recovers. Figure 2 shows the various operational stages of the commercial cellular network and ECN. Upon the disaster occurrence, the commercial cellular network is in failure state: part of MBSs are damaged or out of service. After the first response time, the operator establishes disaster recovery network via deploying a random number of DBSs overlaid the existing cellular network. The DBSs act as a backup for the operational MBSs due to the destruction of cellular infrastructure. Until the deployment of DBSs is finished, the commercial cellular network undergoes partial recovery state.

On the other hand, a network-level restoration process on the commercial network also starts. Disaster failure restoration on cellular networks is often done by dispatching crews to the field to repair directly. All restorations are finished in a random period, since the promptness of failure restoration depends on a combination of various factors, such as environmental constraints,
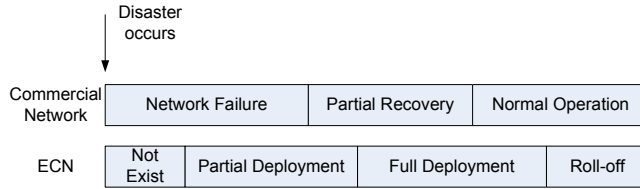
11

Figure 2: Commercial network and ECN operational stages.

preparedness and resources. After the full restoration, the existing cellular network goes back to normal operation. Then the ECN could roll-off. Considering the DBSs are newly deployed, independent random failures and restorations are assumed to occur at individual DBSs.

In order to model the failure and recovery process described above, we introduce a spatial-temporal process as follows,

Definition 2: $\{(N_m(t, \mathcal{A}_0), N_d(t, \mathcal{A}_0)), t \geq 0\}$ is a spatial-temporal process with

$$
\begin{aligned}
N_m(t, \mathcal{A}_0) &= \sum_{1 \leq i \leq N_m; x \in \mathcal{A}_0} \mathbb{I}[X_i(t, x) = 1], \\
N_d(t, \mathcal{A}_0) &= \sum_{1 \leq j \leq N_d; y \in \mathcal{A}_0} \mathbb{I}[X_j(t, y) = 1],
\end{aligned}
\tag{2}
$$

which essentially tells the evolution of total number of operational MBSs and DBSs in region $\mathcal{A}_0$ over time. $\mathbb{I}(A)$ is an indicator function, $\mathbb{I}(A) = 0$ if event A occurs, $\mathbb{I}(A) = 1$ otherwise. We assume for simplicity that each of MBSs and DBSs only have two states: $X_i(t, x) = 0$ if the MBS x is in a failure mode, e.g., no power supply; $X_i(t, x) = 1$ if the MBS x is in normal operation. It is similar case in the operational states of DBSs. N_m and N_d are the maximum possible number of operational MBSs and that of DBSs, respectively. Given the disaster failure occurs at time $t = 0$, then $(N_m(t, \mathcal{A}_0), N_d(t, \mathcal{A}_0))$ defines a stochastic process with state space $\Omega = \{(i, j); i, j \in \mathbb{Z}^+, 0 \leq i \leq N_m, 0 \leq j \leq N_d\}$ to characterize the temporal evolution of recovery of the network.

3. Survivability Analysis

3.1. Survivability of the Network

The objective of the present paper is to quantify the survivability of a cellular network that is subject to disastrous failures. In the evaluation, we adopt the definition of survivability as in [21], which is "the system's ability to continuously deliver services in compliance with the given requirements in the presence of failures and other undesired events".

The network survivability is essentially quantified by the transient performance from the instant when an undesired event occurs until its steady state is reached. As a mathematical description of this temporal process, we adopt the survivability quantification definition given by ANSI-T1A1.2 [20] as illustrated in Figure 3. Let M denote the measure of the performance of interest. The measure M has the value m_0 before a failure occurs. The survivability behavior can be depicted by the following attributes: m_a is the value of M just after the failure occurs; m_u is the maximum difference between the value of M and m_a after the failure; m_r is the restored value of M after some time t_r; and t_R is the relaxation time for the system to restore the value of M [20] [21].
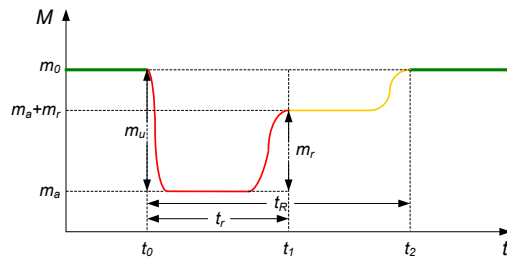

Figure 3: Example of survivability attributes (adapted from [21]).

Note that the model illustrated in Figure 3 is generic. For a specific scenario, in order to evaluate the effectiveness of different survivable designs and mechanisms, it is important to further define what sort of service must be offered, and to specify the performance targets to be achieved. As suggested in [23], the first major goal in survivability of wireless networks is to establish and maintain a

13

connected network, since the breakdown of one BS may affect tens or hundreds of users. Motivated by this, for our work, (i) we define the *service* to be the capacity assigned to users, (ii) the *service requirement* is expressed that the per-user capacity C_u must be higher than a threshold T_C, i.e., $C_u \geq T_C$, and (iii) the *undesired events* are MBSs failure caused by disasters. Accordingly, the measure of performance interest M in the model shown by Figure 3, is the expected per-user capacity for the work of this paper. Specifically, after the failure occurs, m_a denotes the post-disaster value of C_u ; m_r denotes the restored value of C_u after some time t_r; and t_R is the relaxation time for the system to restore the pre-disaster value of C_u [20] [21].

3.2. Average Number of Users under a Operational State

Given the presence of perturbations to the operational state of the network, survivability measures service performance variation during the transient period that starts after a failure till the system fully recovers. However, considering the largeness of state space, it is impossible to measure the performance under different operational state states continuously. In order to limit the number of states, the operational space of the network may be constructed by a finite number of states. For a given set of operational conditions, the network provides a certain level of service. The models with the set of operational states and state transitions during the failure and recovery process will be detailed in subsection 3.3. This subsection discusses how to obtain per-user capacity of the network under a given operational state.

Since MBSs and DBSs follow two different types of distribution, it is better to study the case that the user is associating with MBSs and DBSs, respectively. We denote the users associating with MBSs, DBSs as macrocell users (MUs), deployable cell users (DUs), respectively. The average number of the MU and DU, respectively, are

$$c_m = \mathrm{P}_c^m \lambda_u \lambda_m |\mathcal{A}_0|^2, \tag{3}$$

$$c_d = \mathrm{P}_c^d \lambda_u \lambda_d |\mathcal{A}_0|^2, \tag{4}$$

14

where P_c^m and P_c^d are the coverage probability of an arbitrary user by MBS and DBS, respectively. Thus, the overall average number of users C_u is given by

$$C_u = k_m c_m + k_d c_d \qquad (5)$$

where $k_m = 1 - \exp(-\lambda_m \pi D^2)$ is the fraction of the users served by MBSs, and the rest are served by DBSs.

For cell selection, we assume that the user connects to the BS from which the received power is the highest. Without loss of generality, we will conduct analysis on a typical mobile user located at the origin in our following analysis. The coverage probability of an arbitrary user by the nearest MBS x_0 located at distance r_m is defined as the probability at which the SINR is larger than a pre-defined threshold β_m:

$$\begin{aligned} P_c^m &= \mathbb{P}[\mathrm{SINR}(r_m) > \beta_m] \\ &= \mathbb{P}\left(\frac{P_m h_{r_m} l(r_m)}{I_{r_m} + \sigma^2} > \beta_m \right) \\ &\overset{(a)}{=} \mathcal{L}_{I_{r_m}}\left(\frac{\beta_m}{P_m l(r_m)} \right) e^{\frac{-\beta_m \sigma^2}{P_m l(r_m)}}, \end{aligned} \qquad (6)$$

where (a) follows from Rayleigh fading assumption. Similarly, the coverage probability P_c^d of the arbitrary user by DBS y_0 located at distance r_d can be obtained

$$\begin{aligned} P_c^d &= \mathbb{P}[\mathrm{SINR}(r_d) > \beta_d] \\ &= \mathbb{P}\left(\frac{P_d h_{r_d} l(r_d)}{I_{r_d} + \sigma^2} > \beta_d \right) \\ &= \mathcal{L}_{I_{r_d}}\left(\frac{\beta_d}{P_d l(r_d)} \right) e^{\frac{-\beta_d \sigma^2}{P_d l(r_d)}}. \end{aligned} \qquad (7)$$

In order to further derive the coverage probability P_c^m, P_c^d, we employ the comprehensive study on interference modeling. We consider two spectrum allocation strategies, 1) DBSs have dedicated spectrum band, which is independent from spectrum band of MBSs; 2)MBSs and DBSs share the same spectrum band. These two strategies result in two cases in interference modeling,

- Case 1: Interference only exists in the same tier, rather than across tiers;

- Case 2: Interference exists cross tiers.

3.2.1. Case 1: average user number analysis without cross-tier interference

In the case of without cross-tier interferences, there are two types of interference: the interference from the MBSs to the MUs I_{mm} and the interference from the DBSs to the DUs I_{dd}. Since the MBSs are distributed as a PPP which is stationary, the interference does not depend on the MBS location. Therefore, we denote $\mathcal{L}_{I_{r_m}}$ in Eq. (6) by $\mathcal{L}_{I_{mm}}$, which is

$$
\begin{aligned}
\mathcal{L}_{I_{mm}}(s) &= \mathbb{E}^{!x_0}_{\Phi'_m, h}[\prod_{x \in \Phi'_m} \exp(-sP_m h_x l(x))] \\
&\overset{(a)}{=} \mathbb{E}^{!x_0}_{\Phi'_m}[\prod_{x \in \Phi'_m} \frac{1}{1 + sP_m l(x)}] \\
&\overset{(b)}{=} \exp(-(1-\gamma)\lambda'_m \int_{\mathbb{R}^2 \backslash b(o, r_m)} (1 - \frac{1}{1 + sP_m l(x)}) \mathrm{d}x) \\
&\overset{(c)}{=} \exp(-\pi(1-\gamma)\lambda'_m \frac{(P_m s)^{\frac{2}{\alpha}} G^{-\alpha}}{1 - \frac{2}{\alpha}} r_m^{2-\alpha} F(1, 1 - \frac{2}{\alpha}; 2 - \frac{2}{\alpha}; -P_m s(Gr_m)^{-\alpha})),
\end{aligned}
$$
(8)

where (a) follows from Rayleigh fading assumption, (b) follows from probability generating functional (PGFL) of PPP, and (c) can be obtained with a change to polar coordinates. Substituting Eq. (8) into Eq. (6), P^m_c can be obtained. Similarly, $\mathcal{L}_{I_{dd}}$ is calculated as

$$
\mathcal{L}_{I_{dd}}(s) = \exp(-\pi \widetilde{\lambda}'_d \frac{(P_d s)^{\frac{2}{\alpha}} G^{-\alpha}}{1 - \frac{2}{\alpha}} r_d^{2-\alpha} F(1, 1 - \frac{2}{\alpha}; 2 - \frac{2}{\alpha}; -P_d s(Gr_d)^{-\alpha}). \quad (9)
$$

Substituting Eq. (9) into Eq. (7), P^d_c can be obtained.

3.2.2. Case 2: average user number analysis with cross-tier interference

In this case, there are four types of interference: the interference from the MBSs to the MUs I_{mm}, the interference from the MBSs to the DUs I_{md}, the interference from the DBSs to the MUs I_{dm}, and the interference from the DBSs to the DUs I_{dd}.

The MUs suffer two types of interference: I_{mm} and I_{dm}. The Laplace transform of I_{mm} has been derived in Eq. (8). I_{dm} is stochastically dominated by the interference from the points except those that are within distance D from

16

the desired MBS. Denoting the disk centered at the location of the serving MBS with radius D as H_m, we obtain the Laplace transform of I_{dm} using a modified path loss law $\widetilde{l}(x) = l(x)$, where $x \in \mathbb{R}^2 \backslash H_m$,

$$
\begin{aligned}
\mathcal{L}_{\widetilde{I}_{dm}}(s) &= \mathbb{E}_{\widetilde{\Phi}'_d, h}[\prod_{x \in \widetilde{\Phi}'_d} \exp(-sP_d h_x \widetilde{l}(x))] \\
&= \mathbb{E}_{\widetilde{\Phi}'_d}[\prod_{x \in \widetilde{\Phi}'_d} \frac{1}{1 + sP_d \widetilde{l}(x)}] \\
&= \exp(-\widetilde{\lambda}'_d \int_{\mathbb{R}^2 \backslash b(o, r_m)} (1 - \frac{1}{1 + sP_d l(x)}) \mathrm{d}x) \\
&= \exp(-\widetilde{\lambda}'_d (\frac{(P_d s)^{\frac{2}{\alpha}} 2\pi^2/\alpha}{\sin(2\pi/\alpha)} - \pi D^2 A_m(s, D))),
\end{aligned}
\tag{10}
$$

where

$$
\begin{aligned}
A_m(s, D) &= \frac{1}{\pi D^2} \int_{b(o, r_m)} (1 - \frac{1}{1 + sP_d l(x)}) \mathrm{d}x \\
&= \frac{1}{\pi D^2} \int_0^{2\pi} \int_0^{r_m \cos\varphi + \sqrt{D^2 - r_m^2 \sin^2\varphi}} \frac{r \mathrm{d}r \mathrm{d}\varphi}{1 + (sP_d)^{-1}(Gr)^\alpha}
\end{aligned}
\tag{11}
$$

Independent thinning of Φ'_p outside the exclusive regions with probability $\exp(-\lambda_m \pi D^2)$ yields a good approximation on I_{dm}. Hence, the coverage probability can be approximated as the product of Laplace transform of I_{mm} and I_{dm}.

$$
\mathrm{P}_c^m \approx \mathcal{L}_{I_{mm}}(\frac{\beta_m}{P_m l(r_m)}) \mathcal{L}_{\widetilde{I}_{dm}}(\frac{\beta_m}{P_m l(r_m)})
\tag{12}
$$

Denote the disk centered at the location of the serving DBS with radius D, we have

$$
\mathcal{L}_{I_{md}}(s) = \exp(-\lambda'_d (\frac{(P_d s)^{\frac{2}{\alpha}} 2\pi^2/\alpha}{\sin(2\pi/\alpha)} - \pi D^2 A_d(s, D))),
\tag{13}
$$

where

$$
A_d(s, D) = \frac{1}{\pi D^2} \int_0^{2\pi} \int_0^{r_d \cos\varphi + \sqrt{D^2 - r_d^2 \sin^2\varphi}} \frac{r \mathrm{d}r \mathrm{d}\varphi}{1 + (sP_m)^{-1}(Gr)^\alpha}
\tag{14}
$$

Similar to the interference to the MUs, the DU also experiences two types of interference: I_{md} and I_{dd}. The coverage probability of DU can be approximated

17

as the product of Laplace transform of I_{md} and I_{dd}.

$$\mathrm{P}_c^d \approx \mathcal{L}_{I_{md}}(\frac{\beta_d}{P_d l(r_d)}) \mathcal{L}_{\widetilde{I}_{dd}}(\frac{\beta_d}{P_d l(r_d)}) \tag{15}$$

The number/density of operational MBSs and DBSs in $\mathcal{A}_0$ might determine
the network performance, including coverage probability and per-user capaci-
ty. In the next subsection, a Markov chain based analysis on operational state
$\{(N_m(t, \mathcal{A}_0), N_d(t, \mathcal{A}_0)), t \geq 0\}$ is established, with which how the per-user ca-
pacity and service unavailability evolves over time after the occurrence of the
disaster is further derived in the subsection afterwards.

3.3. Markov Chain Analysis on the Numbers of Operational BSs over Time

In this subsection, we detail the phased recovery model, where each phase
may have different set of available resources for the wireless access. It charac-
terizes the set of operational states during the transient period that starts after
a failure till the system fully recovers. We assume that the state holding times
are exponentially distributed, which serves to illustrate our model analysis in a
simple setting. Extending the model to allow for general distributions for the
state holding times is left as future work. Formally, when used in modeling, the
assumptions are characterized as:

- The system suffers disastrous breakdown resulting in part of MBSs out
  of-service. After the disaster occurrence, the operator establishes disaster
  recovery network via deployment of a random number of DBSs overlaid
  the existing cellular network. It is followed by a full restoration process
  on the MBSs. All the state holding times are exponentially distributed.

- DBSs have independent transient failures according to Poisson processes
  with rate ν. The transient failure of each DBS can be recovered shortly and
  the recovery time for DBSs is exponentially distributed with parameter μ.

The sequence of phases are described as a continuous-time Markov chain
(CTMC) model to characterize the transient network response behavior, in

18

terms of numbers of operational MBSs and DBSs in the system, after the dis-

350 aster until the system stabilizes again. The state transition diagram of this Markov chain is illustrated in Figure 4. In Figure 4 the life cycle of the failure and restoration is described in four phases, $y = \text{I, II, III, IV}$, which represent four operational stages of ECN: no exist, partial deployment, full deployment and roll-off. The composite CTMC state (y, i, j) constitutes of the phase y, the

355 number of operational MBSs i and the number of operational DBSs j. The transition from state (y, i, j) to state $(y, i, j-1)$ denotes a transient failure of one DBS. The corresponding transition rate is $j\nu$. The transition from state $(y, i, j-1)$ to state (y, i, j) denotes the transient recovery of one DBS with mean rate μ.

Note that for survivability analysis, our focus is on the system's transient behavior after the disaster. For this reason, disastrous failure is forced (dashed arc in Figure 4). The various transition rates $q_{(y,i,j),(y',i',j')}$ of the CTMC are

$$q_{(y,i,j),(y,i,j-1)} = j\nu, \quad y = \text{II, III}, i = \{(1-\gamma)N_m, N_m\}, j = 0, 1, \cdots, N_d$$

$$q_{(y,i,j-1),(y,i,j)} = \mu, \quad y = \text{II, III}, i = \{(1-\gamma)N_m, N_m\}, j = 0, 1, \cdots, N_d$$

$$q_{(\text{II},(1-\gamma)N_m,j),(\text{III},N_m,j)} = \tau_f, \quad j = 0, 1, \cdots, N_d \quad (16)$$

$$q_{(\text{I},(1-\gamma)N_m,0),(\text{II},0,N_d)} = \tau_p$$

$$q_{(\text{III},N_m,N_d),(\text{IV},N_m,0)} = \tau_r$$

360 Based on the above transition rate regulations, the state transition rate matrix of this model can be obtained as $\mathbf{Q} = [q_{(y,i,j),(y',i',j')}]$.

3.4. Service Unavailability over Time

To facilitate the representation, we denote the per-user capacity under a given system state (y, i, j) as $C_{(y,i,j)}(t)$. It can be viewed as a reward process on

365 the CTMC model $\{N_m(t, \mathcal{A}_0), N_d(t, \mathcal{A}_0)\}$, whose analysis has been established in the previous subsection.

Let $P(t) = [P_{(I,0,0)}(t) \cdots P_{(y,i,j)}(t) \cdots P_{(IV,N_1,0)}(t)]$ denote a row vector of transient state probabilities at time t. In order to calculate $P(t)$, the Kolmogorov-forward equation expressed in the matrix form should be satisfied as follows:
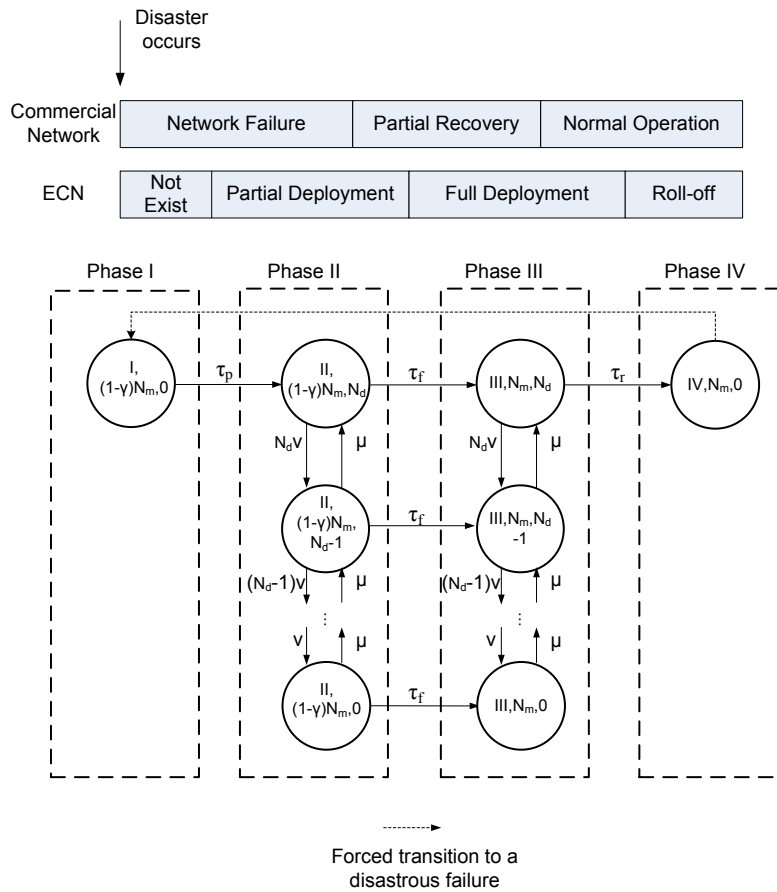
19

Figure 4: State transition diagram for the network operational stages.

$$\frac{dP(t)}{dt} = P(t)\mathbf{Q} \tag{17}$$

where $\mathbf{Q}$ is the transition rate matrix. Then the transient state probability vector can be obtained as follows:

$$P(t) = e^{\mathbf{Q}t} \tag{18}$$

where $e^{\mathbf{Q}t}$ is defined as follows:

$$e^{\mathbf{Q}t} = \sum_{i=0}^{\infty} \mathbf{Q}^i \frac{t^i}{i!} \tag{19}$$

The simplest method to compute Eq. (19) is to truncate the summation to a large number (e.g., K), which can be expressed as follows:

$$e^{\mathbf{Q}t} = \sum_{i=0}^{K} \mathbf{Q}^i \frac{t^i}{i!} \tag{20}$$

An alternative way to compute the transient probabilities is by using eigenvalues. In this method, $\mathbf{Q}$ is assumed to be diagonalizable,

$$\mathbf{Q} = \mathbf{U}\mathbf{V}\mathbf{U}^{-1} \tag{21}$$

where $\mathbf{V}$ is a diagnoal matrix of eigenvalues. The transient probabilities can be defined as follows:

$$\mathbf{V} = \begin{bmatrix} e^{v_1 t} & & & \\ & e^{v_2 t} & & \\ & & \ddots & \\ & & & e^{v_N t} \end{bmatrix}$$

Then, the transition probabilities can be written as follows:

$$P(t) = \mathbf{U}(\sum_{i=0}^{\infty} \mathbf{V}\frac{t^i}{i!})\mathbf{U}^{-1}$$

$$\tag{22}$$

$$= \mathbf{U}e^{\mathbf{V}t}\mathbf{U}^{-1}$$

Finally, combining the above calculated transient probabilities $P_{(y,i,j)}(t)$ and average number of users associated with each state $C_{(y,i,j)}(t)$, the expected instantaneous reward rate $E[C(t)]$ gives the expected number of users at time t, which is expressed as follows:

$$E[C(t)] = \sum_{y=\mathrm{I}}^{\mathrm{IV}} \sum_{i,j} C_{(y,i,j)}(t) P_{(y,i,j)}(t). \tag{23}$$

3.4.1. Product-Form Approximation

370   The above so-called exact modeling approach for calculating the transition probabilities needs to visit each state and to repeat the transient state analysis, which could be computational challenging when the network size is large. As a result, such transient analysis can be too complex for a symbolic closed-form solution, and even too difficult for a numerical solution.

Since the transient failures and repairs of two classes of BSs are independent, we can apply an approximation to facilitate the calculation of the transient probability $P_{(y,i,j)}(t)$ for state (y,i,j). This is a product-form approach as follows:

$$P_{(y,i,j)}(t) = P(t,i) \cdot \pi(y,j) \tag{24}$$

375   where $P(t,i)$ is the transient probability of a state i $(0 \leq i \leq N_1)$, and $\pi(j)$ is the steady state probability of a state j $(0 \leq j \leq N_2)$.

To calculate the steady state $\pi(j)$, the equilibrium state equations are used:

$$\pi(0)\mu = \pi(1)\nu$$

$$\pi(0)\mu + 2\pi(2)\nu = \pi(1)(\mu + \nu)$$

$$\vdots$$

$$\pi(N_2 - 1)\mu = N_2 \pi(N_2)\nu$$

With μ and ν, the closed-form steady state probability $\pi(j)$ can be derived:

$$\pi(j) = \frac{1}{j!} (\frac{\mu}{\nu})^j \pi(0) \tag{25}$$

22

Table 2: System Parameter Setting

Notation	Description
$\mathcal{A}_0$	$2.5 \times 1.9 (km^2)$
λ_m	$0.95 (1/km^2)$
λ_d	$1.9 (1/km^2)$
λ_u	$5 (1/km^2)$
γ	0.1
P_m, P_d	43dbm,30dbm
β_m, β_d	5dB,5dB
α	4
G	$6910 (km^{-1})$

where $\pi(0)$ is obtained according to the normalization condition $\sum_{j=0}^{N_2} \pi_j = 1$,

$$\pi(0) = \frac{1}{\sum_{k=0}^{N_2} \frac{1}{k!} (\frac{\mu}{\nu})^k} \tag{26}$$

Then, the expected number of connected users $E[C(t)]$ becomes:

$$E[C(t)] = \sum P(t, i) \cdot \pi(j) \tag{27}$$

As a highlight, the product-form approach requires only transient solution of evolution of macrocell BSs and the steady-state solution of evolution of small cell BSs.

4. Results

In this section, the assumptions used in the proposed survivability quantification models are first validated, before results and insights from numerical experiments are presented.

4.1. Validity of Model Accuracy

In this subsection, the decomposition assumption used in the proposed survivability quantification models is validated.

23

Table 3: Failure/Recovery Rate Parameter Setting

Parameter	Value
τ_p	$10(hour^{-1})$
τ_f	$10(hour^{-1})$
τ_r	$0.2(hour^{-1})$
ν	$20(hour^{-1})$
μ	$10(hour^{-1})$

4.1.1. Validity of the Equations in Section 3.2

Figure 5 shows the variations of coverage probability with respect to the SINR thresholds. It can observed in 5(a) that the MU coverage probability decreases with the increasing SINR threshold θ_m and in 5(b) that the DU coverage probability decreases with the increasing SINR threshold θ_d. We can observe that the bounds derived for the coverage probability of both types of users are quite tight and the approximation matches the simulation result very well.

The effects of different range expansion bias ζ are also shown in Figure 5(a) and 5(b). In Figure 5(a), we find that the larger of ζ, the lower coverage probability of MUs. We can clearly also notice the performance degradation in Fig. 5(b) for higher values of γ. On the other hand, ζ affects the performance of the DUs less strongly than that of the MUs. This is because ζ has a direct effect on the exclusion radius D, which determines the number of users accessing the MBS.

The average number of connected users as a function of the damage ratio γ is shown in Figure 6(a) and 6(b), with different densities λ_d of DBSs. These results show that the average number of users in Eq. (5) decreases with the increasing damage ratio γ. This observation suggests that the number of operational MBSs has a pronounced effect on the user performance. These results also show that the performance improves with more number of DBSs.
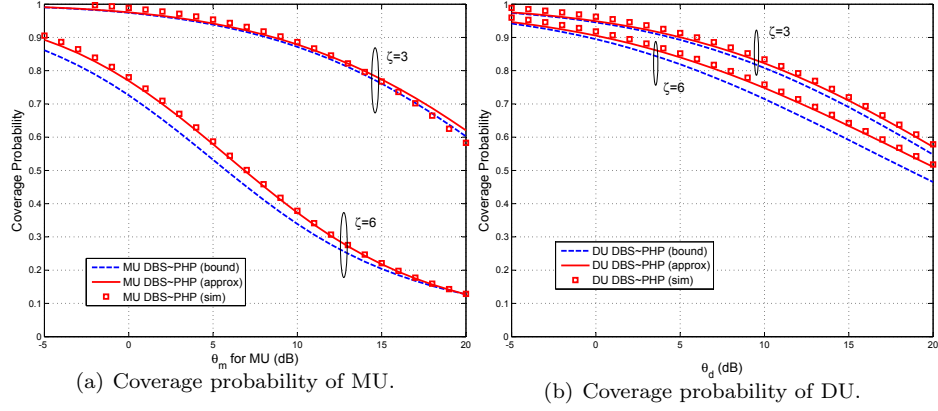
24

(a) Coverage probability of MU.

(b) Coverage probability of DU.

Figure 5: Effects of cell range expansion bias on coverage probability (Case 2).

(a) Validation of case 1: Eq. (89).
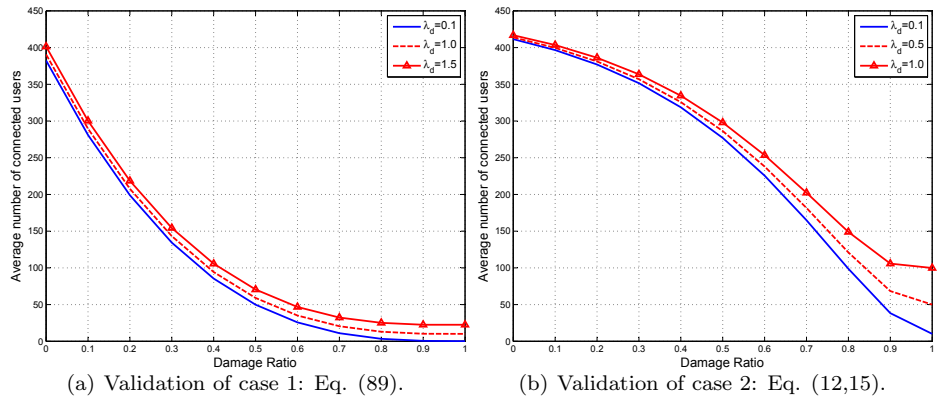
(b) Validation of case 2: Eq. (12,15).

Figure 6: Effects of damage ratio on average number of connected users.

4.1.2. Validity of the Decomposition Assumption

We validate the decomposition assumption used in our proposed product-form modeling approach. Table 2 lists the default value of system parameters. Consider one urban area $\mathcal{A}_0$ with $2.5 * 1.9 (/km * km)$ covered by a two-tier infrastructure-based wireless network. The density of two tiers BSs are $\lambda_m = 0.95(/km^2), \lambda_d = 1.9(/km^2)$, respectively. The density of users in $\mathcal{A}_0$ is $\lambda_u = 100(/km^2)$. The maximum number of operational BSs can be estimated as $N_1 = \lambda_1|\mathcal{A}_0|$, $N_2 = \lambda_2|\mathcal{A}_0|$. The transmit power of two tiers BSs are $P_1 = 43(dbm), P_2 = 37(dbm)$, respectively. We set $\alpha = 3.8$ and $K = 6910km^{-1}$ (which corresponds to the COST Walfisch-Ikegami model for urban environment) [24]. It is a natural assumption to say that the transient failure/recovery rates are larger than the network-level full restoration rate.

We verify the decomposition assumption by considering the system failure/recovery parameters setting in two scenarios: 1) a small scale network in area $|\mathcal{A}_0| = 2.5*1.9$ with parameter ($\nu = 2, \mu = 10, \tau = 0.2$), 2) a relatively larger scale network in area $|\mathcal{A}_0| = 3.4*2.8$ with parameter ($\nu = 3, \mu = 15, \tau = 0.2$). As shown in Figures 7(a) and 7(b), the product-form approach and the exact approach results match reasonably well for different parameter settings. This comparison shows that the decomposition assumption is accurate in the case of spatial independence existing between the two BSs tiers of the network.

We examine the way in which parameter τ affects the survivability model. Comparing to the smooth curve of service unavailability $E[C(t)]$ when $\tau = 0.08(\text{hour}^{-1})$, the curves of service unavailability when $\tau = 0.8(\text{hour}^{-1})$ reach the steady state faster. This difference in curves' trend reflects the impact of τ on service unavailability: τ is larger, then service unavailability decreases to 0 faster. In other words, faster global repair may bring the networked system back to pre-disaster level in a shorter period of time.

First, we consider a small network case $|\mathcal{A}_0| = 3.4 * 2.8(km^2)$. We plot the quantification results as shown in Figure 8(a), solid curves represent the results of product-form model approach while the dashed curves are the results
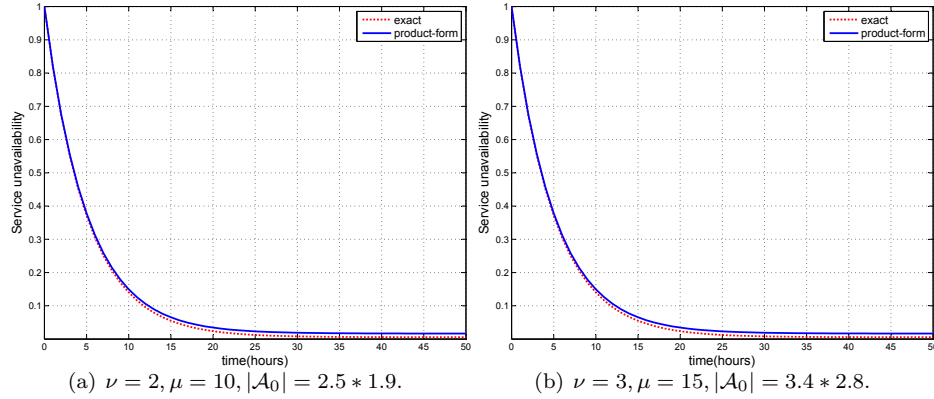
26

(a) $\nu = 2, \mu = 10, |\mathcal{A}_0| = 2.5 * 1.9.$ (b) $\nu = 3, \mu = 15, |\mathcal{A}_0| = 3.4 * 2.8.$

Figure 7: Validation of the decomposition assumption ($\tau = 0.2, \nu_1 = 1, \mu_1 = 20$).

of exact model approach. As this figure suggests, the survivability quantification notations are displayed as m_a, t_R, m_0 and the curves decrease with time elapse as expected .

440   Then we extend the analysis to a larger network case $|\mathcal{A}_0| = 5 * 2.9(km^2)$. The survivability quantification results m_a, t_R, m_0 are shown as the notations as in Figure 8(b). Similar observations can be found that the curves of service unavailability with larger τ reach the steady state faster. Since the mean time for a global repair is much longer than the mean repair time of one access point 445 is obvious, it is naturally assumed that τ is much less than μ.

     Comparing to Figure 7, there exists a more noticeable small difference gap between the two curves of both approaches in Figure 8(a) and 8(b). This is due to that the decomposition in the product-form approach is based on the assumption that the transient failures and repairs of two types of BSs are inde-450 pendent. In addition, in the decomposition approach analysis, we have assumed during the transient failure/recovery of tier 1 BSs, tier 2 BSs' operation states have reached steady state. Nevertheless, the observation in Figure 8(a) and 8(b) demonstrates that the product-form approach, though not exactly accurate, appealingly provides a tight lower bound to the exact approach.
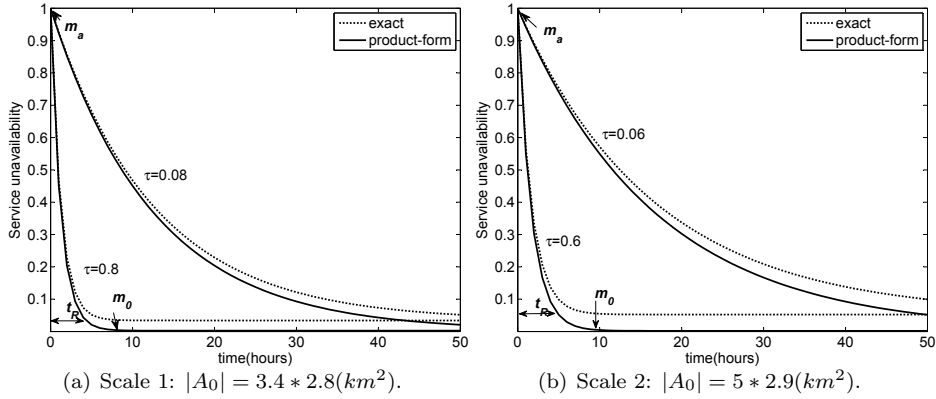
27

(a) Scale 1: $|A_0| = 3.4 * 2.8 (km^2)$.   (b) Scale 2: $|A_0| = 5 * 2.9 (km^2)$.

Figure 8: Log-plot of service unavailability $E[U(t)]$ versus time t.

4.2. Numerical Results

In this subsection, we attempt to gain more insights from numerical experiments which were run using Mathematica [25]. First, to demonstrate the applicability of the proposed product-form solution, we compare it with the exact model approach in terms of performance and scalability. Then we examine the effect of different model parameters on the defined performance measures.

4.2.1. Computational Complexity Analysis

To show the computational advantages of the product-form approach over the exact model approach, we compare the time needed for calculating the transient probabilities using the two approaches. We run experiments with three network scales (case 1: $N_1 = 2, N_2 = 2$; case 2: $N_1 = 3, N_2 = 2$; case 3: $N_1 = 3, N_2 = 3$). Note that here we choose these N_1, N_2 ideal values only for testing the computational speed. The other parameters are chosen as $\nu = 0.005, \mu = 2, \tau = 0.02$. In all the experiment cases, 30 runs are performed and the mean running time (unit: seconds) are recorded as shown in Table 4.

The observation from Table 4 suggests that the product-form approach is able to almost immediately give the transient probabilities. However, it may take about 0.6 seconds by using the exact model approach in case 1. Similar results can be obtained from experiments case 2 and case 3. For the exact

28

model approach, it takes more time (about 2 seconds in case 2 and 8 seconds in case 3) than in case 1. The growing of network size has significant impact on the computational complexity of the exact model approach. The product-form approach reduces the state space of the transient solution as indicated in Equation (27). This explains why the product-form approach has advantages in transient solution computation than the exact model approach. For large-scale networks, it can be expected that the exact model approach will be more time consuming in transient solution computation while the product-form approach may then be preferred.

4.2.2. Impact of Parameters on Survivability Performance

In the following, both approaches are used to numerically obtain the system survivability performance. The system parameters are chosen as: $\nu = 2(hour^{-1}), \mu = 10(hour^{-1}), P_1 = 43(dbm), P_2 = 37(dbm), \alpha = 3.8, \lambda_1 = 0.95(/km^2), \lambda_2 = 1.9(/km^2), \lambda_u = 100(/km^2)$.

In brief, compared with the exact model approach which is preferred for small size models, the product-form approach is more scalable with reasonably good accuracy and hence may be more preferred for analysis of large size networks.

5. Conclusion

We have conducted analysis on the survivability of a two-tier heterogeneous infrastructure wireless network that is subject to disastrous breakdowns. The focus has been on the transient behavior of the network under disastrous fail-

Table 4: Comparison of computational time for transient probabilities using the two approaches under three cases (mean ± standard error, unit: seconds).

	case 1	case 2	case 3
Exact	0.581 ± 0.316	1.997 ± 0.890	7.899 ± 0.895
Product-form	0.021 ± 0.017	0.041 ± 0.026	0.041 ± 0.016

29

ures, of which a continuous-time Markov chain (CTMC) model is established. Detailed analysis has been performed based on the CTMC model. In the analysis, the location of BSs and users are considered, by modeling their distributions with Poisson point processes (PPPs). In addition, to help reduce the computation complexity, a product-form spatial decomposition approach is introduced. The Poisson point process (PPP) assumption and the product-form decomposition assumption are validated on real data. Moreover, numerical experiments have been performed to study the approximation accuracy and computational efficiency of the product-form analysis approach against the exact analysis. The results show that the product-form approximation provides tractable and reasonably accurate analysis. In addition, the numerical results have also examined the impact of different parameters on the network's survivability.

As another concluding remark, we highlight that, the recovery time in the current model has for simplicity been assumed to be exponentially distributed which may not be true in real scenario. More general model, such as phase-type model or semi-Markov model may be used. In addition, this paper considers a static disaster failure scenario, where all affected macro BSs in one geographical area are assumed to fail simultaneously. In reality, disasters may not be static. For example, a hurricane usually has a landfall with a strong force wind, and then gradually fades down when moving in land. As a result, the affected network components might fail progressively over time due to the influence of disaster spreading, rather than being out of operation at the same time. Our future work will attempt to characterize such dynamic nature of failures and recoveries due to evolution of external disturbances in the survivability model.

References

[1] A. Kwasinski, W. Weaver, P. Chapman, P. Krein, Telecommunications power plant damage assessment for hurricane katrina - site survey and follow-up results, IEEE Systems Journal 3 (3) (2009) 277–287.

[2] T. Adachi, Y. Ishiyama, Y. Asakura, K. Nakamura, The restoration of

telecom power damages by the great east japan earthquake, in: Proceedings
₅₂₅ of the IEEE Telecommunication Energy Conferenc, 2011.

[3] https://en.wiki2.org/wiki/cyclone_dagmar.

[4] T. Sakano, S. Kotabe, T. Komukai, T. Kumagai, Y. Shimizu, A. Takahara,
T. Ngo, Z. M. Fadlullah, H. Nishiyama, N. Kato, Bringing movable and
deployable networks to disaster areas: development and field test of mdru,
₅₃₀ IEEE Network 30 (1) (2016) 86–91. `doi:10.1109/MNET.2016.7389836`.

[5] R. Li, X. Wang, X. Jiang, Network survivability against region failure,
in: Proceedings of IEEE International Conference on Signal Processing,
Communications and Computing, 2011, pp. 1–6. `doi:10.1109/ICSPCC.`
`2011.6061633`.

₅₃₅ [6] O. Diaz, F. Xu, N. Min-Allah, M. Khodeir, M. Peng, S. Khan, N. Ghani,
Network survivability for multiple probabilistic failures, IEEE Communica-
tions Letters 16 (8) (2012) 1320–1323. `doi:10.1109/LCOMM.2012.060112.`
`120353`.

[7] B. Bassiri, S. S. Heydari, Network survivability in large-scale regional fail-
₅₄₀ ure scenarios, in: Proceedings of the 2nd Canadian Conference on Com-
puter Science and Software Engineering, 2009, pp. 83–87. `doi:10.1145/`
`1557626.1557639`.

[8] S. Neumayer, G. Zussman, R. Cohen, E. Modiano, Assessing the vulner-
ability of the fiber infrastructure to disasters, IEEE/ACM Trans. Netw.
₅₄₅ 19 (6) (2011) 1610–1623. `doi:10.1109/TNET.2011.2128879`.

[9] P. K. Agarwal, A. Efrat, S. K. Ganjugunte, D. Hay, S. Sankararaman,
G. Zussman, Network vulnerability to single, multiple, and probabilistic
physical attacks, in: Proceedings of Military Communications Conference,
2010, pp. 1824–1829. `doi:10.1109/MILCOM.2010.5679556`.

₅₅₀ [10] S. Trajanovski, F. A. Kuipers, A. Ili, J. Crowcroft, P. V. Mieghem, Finding
critical regions and region-disjoint paths in a network, IEEE/ACM Trans-

actions on Networking 23 (3) (2015) 908–921. `doi:10.1109/TNET.2014.2309253`.

[11] D. L. Msongaleli, F. Dikbiyik, M. Zukerman, B. Mukherjee, Disaster-aware submarine fiber-optic cable deployment, in: Proceedings of Optical Network Design and Modeling (ONDM), 2015, pp. 245–250. `doi:10.1109/ONDM.2015.7127306`.

[12] M. Haenggi, Stochastic Geometry for Wireless Networks, Cambridge University Press, 2012.

[13] J. Andrews, F. Baccelli, R. Ganti, A tractable approach to coverage and rate in cellular networks, IEEE Transactions on Communications 59 (11) (2011) 3122–3134. `doi:10.1109/TCOMM.2011.100411.100541`.

[14] H. Dhillon, R. Ganti, F. Baccelli, J. Andrews, Modeling and analysis of k-tier downlink heterogeneous cellular networks, IEEE Journal on Selected Areas in Communications 30 (3) (2012) 550–560. `doi:10.1109/JSAC.2012.120405`.

[15] J. G. Andrews, S. Buzzi, W. Choi, S. V. Hanly, A. Lozano, A. C. K. Soong, J. C. Zhang, What will 5g be?, IEEE Journal on Selected Areas in Communications 32 (6) (2014) 1065–1082. `doi:10.1109/JSAC.2014.2328098`.

[16] H. Zhang, C. Jiang, R. Q. Hu, Y. Qian, Self-organization in disaster-resilient heterogeneous small cell networks, IEEE Network 30 (2) (2016) 116–121. `doi:10.1109/MNET.2016.7437033`.

[17] P. V. Mekikis, E. Kartsakli, A. Antonopoulos, A. S. Lalos, L. Alonso, C. Verikoukis, Two-tier cellular random network planning for minimum deployment cost, in: 2014 IEEE International Conference on Communications (ICC), 2014, pp. 1248–1253. `doi:10.1109/ICC.2014.6883492`.

[18] N. Deng, W. Zhou, M. Haenggi, Heterogeneous cellular network models with dependence, IEEE Journal on Selected Areas in Communications 33 (10) (2015) 2167–2181. `doi:10.1109/JSAC.2015.2435471`.

[19] V. Jindal, S. Dharmaraja, S. Kishor, Analytical survivability model for fault tolerant cellular networks supporting multiple services, in: Proceedings of the IEEE International Symposium on Performance Evaluation of Computer and Telecommunication Systems, 2006, pp. 505–512.

[20] Technical report on enhanced network survivability performance, Tech. Rep. 68, ANSI T1A1.2 Working Group on Network Survivability Performance (2001).

[21] P. E. Heegaard, K. S. Trivedi, Network survivability modeling, Comput. Netw. 53 (2009) 1215–1234. `doi:10.1016/j.comnet.2009.02.014`.

[22] B. Blaszczyszyn, M. K. Karray, Linear-Regression Estimation of the Propagation-Loss Parameters Using Mobiles' Measurements in Wireless Cellular Networks, in: WiOpt'12: Modeling and Optimization in Mobile, Ad Hoc, and Wireless Networks, Paderborn, Germany, 2012, pp. 54–59, cellular Networks.
URL `https://hal.inria.fr/hal-00763309`

[23] J. P. G. Sterbenz, R. Krishnan, R. R. Hain, A. W. Jackson, D. Levin, R. Ramanathan, J. Zao, Survivable mobile wireless networks: issues, challenges, and research directions, in: Proceedings of the 1st ACM workshop on Wireless security, 2002, pp. 31–40. `doi:10.1145/570681.570685`.

[24] H. P. Keeler, B. Baszczyszyn, M. K. Karray, Sinr-based k-coverage probability in cellular networks with arbitrary shadowing, in: 2013 IEEE International Symposium on Information Theory, 2013, pp. 1167–1171. `doi:10.1109/ISIT.2013.6620410`.

[25] http://reference.wolfram.com/mathematica/guide/mathematica.html.